Thieme

Morphology of Retinal Hemangioblastoma in von Hippel-Lindau Disease Revealed by Optical Coherence Tomography Angiography

Morphologie von retinalen Hämangioblastomen bei Von-Hippel-Lindau-Erkrankung dargestellt durch optische Kohärenztomografie-Angiografie

OPEN ACCESS

Authors
Yannik Laich[1], Stefan J. Lang[2], Andreas Glatz[1], Navid Farassat[1], Felicitas Bucher[1], Simone Nuessle[1], Daniel Böhringer[1], Wolf Alexander Lagrèze[1], Spyridon Sideris[3], Peter Maloca[4,5], Clemens Lange[1,6], Thomas Reinhard[1], Hansjürgen Agostini[1], Michael Reich[1,7]

Affiliations
1 Eye Center, Medical Center - University of Freiburg, Faculty of Medicine, Freiburg, Germany
2 Department of Ophthalmology, University Hospital Brandenburg, Brandenburg Medical School, Brandenburg an der Havel, Germany
3 Jules Bordet Institute, Medical Oncology Department, University Hospital of Brussels, Brussels, Belgium
4 Medical Practice for Ophthalmology Priv.-Doz. Dr. med. Peter Maloca, Luzern, Switzerland
5 Moorfields Eye Hospital NHS Foundation Trust, London, United Kingdom
6 Ophtha-Lab, Department of Ophthalmology at St. Franziskus Hospital, Muenster, Germany
7 Augenärzte am Städel, Medical Practice for Ophthalmology, Frankfurt am Main, Germany

Keywords
retinal hemangioblastoma, morphology, von Hippel-Lindau disease, optical coherence tomography angiography, OCTA

Schlüsselwörter
retinale Hämangioblastome, Morphologie, Von-Hippel-Lindau Erkrankung, optische Kohärenztomografie-Angiografie, OCTA

received	3.11.2024
accepted	25.11.2024
published online	2025

Bibliography
Klin Monatsbl Augenheilkd 2025
DOI 10.1055/a-2501-8628
ISSN 0023-2165

Georg Thieme Verlag KG, Oswald-Hesse-Straße 50, 70469 Stuttgart, Germany

Correspondence
Dr. Michael Reich, M. D.
Augenärzte am Städel
Hans-Thoma-Strasse 24, 60596 Frankfurt am Main, Germany
Phone: + 49 (0) 69 96 23 72 90, Fax: + 49 (0) 69 96 23 72 92
drmichaelreich@web.de

Supplementary Material is available under: https://doi.org/10.1055/a-2501-8628

ABSTRACT

Background To characterize different growth patterns of retinal hemangioblastomas (RHs) in patients with von Hippel-Lindau disease (VHLD) using swept-source optical coherence tomography angiography (SS-OCTA).

Methods Single-center observational cross-sectional study. SS-OCTA B-scans were centered over primary treatment-naïve RHs to display the perfusion in the inner, middle, and outer areas (IA, MA, OA). Distinctive growth patterns were characterized using K-means cluster analysis of the flow signal.

Results Annual screening of 201 patients with VHLD revealed 49 patients with 85 RHs (41 recurrent, 44 primary treatment-naïve RHs). High-quality SS-OCTA images were available for 24 primary RHs and were pooled with scans of the treatment-naïve form of 6 recurrent RHs, which were taken at a prior visit, for further analysis. Out of 30 primary RHs, 18 were located juxtapapillary (jRH) and 12 peripherally (pRH). K-means cluster analysis distinguished seven exophytic (23.3%, 2 jRH, 5 pRH), nine endophytic (30%, 6 jRH, 3 pRH), and fourteen sessile (46.7%, 10 jRH, 4 pRH) growth patterns. Fractions of the flow signal in the IA, MA, and OA were 7.3 ± 3.3%, 89.3 ± 5.0%, and 3.4 ± 3.5% for exophytic RHs, 22.2 ± 7.4%, 65.6 ± 7.3%, and 12.1 ± 8.2% for sessile RHs, and 65.4 ± 5.7%, 26.6 ± 4.9%, and 8.0 ± 6.1% for endophytic RH.

Conclusion OCTA contributes to further elucidating the morphology of RHs as a useful complementary diagnostic tool that can help to provide customized therapeutic ap-

proaches in the future and thus improve the effectiveness of RH treatment.

ZUSAMMENFASSUNG

Hintergrund Ziel der Studie ist die Charakterisierung unterschiedlicher Wachstumsmuster von retinalen Hämangioblastomen (RHs) bei Patienten mit Von-Hippel-Lindau-Krankheit (VHLD) mittels Swept-Source optischer Kohärenztomografie-Angiografie (SS-OCTA).

Methoden Monozentrische Querschnittsstudie. SS-OCTA-B-Scans von primären, unbehandelten RHs wurden erstellt, um die Perfusion in den inneren, mittleren und äußeren Bereichen (IA, MA, OA) der RH darzustellen. Charakteristische Wachstumsmuster wurden mithilfe einer K-Means-Cluster-Analyse des Flusssignals ermittelt.

Ergebnisse Bei jährlichen Screenings von 201 Patienten mit VHLD wurden bei 49 Patienten 85 RHs (41 rezidivierende, 44 primäre, unbehandelte RHs) detektiert. SS-OCTA-Scans von 24 primären RHs wurden zusammen mit Aufnahmen der unbehandelten Form von 6 rezidivierenden RHs, die bei einem früheren Besuch erhoben wurden, zur weiteren Analyse zusammengeführt. Von den 30 primären RHs waren 18 juxtapapillär (jRH) und 12 peripher (pRH) gelegen. Mittels K-Mittel-Cluster-Analyse wurden sieben exophytische (23,3 %, 2 jRH, 5 pRH), 9 endophytische (30 %, 6 jRH, 3 pRH) und 14 sessile (46,7 %, 10 jRH, 4 pRH) Wachstumsmuster unterschieden. Die jeweiligen Anteile des Flusssignals in der IA, MA und OA betrugen 7,3 ± 3,3 %, 89,3 ± 5,0 %, 3,4 ± 3,5 % für exophytische RHs, 22,2 ± 7,4 %, 65,6 ± 7,3 %, 12,1 ± 8,2 % für sessile RHs und 65,4 ± 5,7 %, 26,6 ± 4,9 %, 8,0 ± 6,1 % für endophytische RHs.

Schlussfolgerung Die OCTA bietet als ergänzendes diagnostisches Verfahren einen wertvollen Beitrag zur weiteren Aufklärung der Morphologie von RHs. Sie kann zukünftig zur Entwicklung individuellerer therapeutischer Ansätze beitragen und dadurch die Effektivität der Behandlung von RH bei VHLD verbessern.

List of Abbreviations

RH	retinal hemangioblastoma
VHLD	von Hippel-Lindau disease
SS-OCTA	swept-source optical coherence tomography angiography
jRH	juxtapapillary retinal hemangioblastoma
pRH	peripherally retinal hemangioblastoma
IA, MA, OA	inner, middle, and outer area
ONL	outer nuclear layer
RPE	retinal pigment epithelium
IPL	inner plexiform layer
ILM	internal limiting membrane
FA	fluorescein angiography
SS-OCT	swept-source OCT
SD	spectral domain
StD	standard deviation

Background

Von Hippel-Lindau disease (VHLD) is a rare autosomal dominant inherited phacomatosis [1–3] characterized by the development of vascular tumors or cysts in various organ systems [4–7], most commonly, hemangioblastomas in the brain and retina [4–7]. Retinal hemangioblastoma (RH) occurs in 50 to 70 % of VHLD patients [8–10], with an increasing prevalence with age, affecting 90 % of those patients over 60 years [11–14].

Clinically, RHs appear as reddish, spherical, vascular lesions in the peripheral retina (pRH) and – more rarely – in the juxtapapillary area (jRH) [15, 16]. Morphologically, three different growth patterns of pRH and jRH have been described in regards to the localization in the retina [17]: exophytic, sessile, and endophytic (Supplemental Fig. 1). Exophytic RHs are nodular, reddish or orange-colored lesions and grow in the outer layers of the retina (between the outer nuclear layer [ONL] and retinal pigment epithelium [RPE]). Sessile RHs are relatively flat, gray, orange, or reddish in color, and develop in the middle layer of the retina (between halfway to the inner plexiform layer (IPL) and ONL). Endophytic RHs grow on the surface of the optic nerve or retina between the internal limiting membrane (ILM) and halfway to the IPL. Endophytic RHs may protrude into the vitreous cavity [17, 18].

Despite their benign nature in general, RHs can cause subretinal fluid or retinal traction, resulting in visual impairment if left untreated [8]. Early detection through regular monitoring and appropriate treatment can significantly impact the visual prognosis [8]. Depending on tumor location, size, and morphology, treatment options for RHs include observation, off-label use of belzutifan [19], thermal laser photocoagulation, photodynamic therapy, cryotherapy, radiotherapy, and vitreoretinal surgery.

Conventional ophthalmic screening examinations, including ophthalmoscopy and fundus photography, often fail in detecting smaller RHs [20, 21]. Fluorescein angiography (FA) shows a higher detection rate of RHs than clinical examination alone but is an invasive diagnostic tool [22]. Furthermore, optical coherence tomography angiography (OCTA) has been proposed as a noninvasive tool for early detection of RHs, monitoring their progression, and evaluating treatment efficacy [20, 21]. OCTA is based on motion contrast to image blood flow, with no need for an intravascular dye injection [22]. A new generation of OCTA uses a swept-source OCT (SS-OCT) system, which allows a deeper tissue penetration with a faster acquisition time compared to older spectral-domain (SD) OCTA generations [23]. Hence, SS-OCTA is able to reduce shadowing artifacts due to subretinal fluid better than SD-OCTA [24] and might therefore be preferred when imaging RHs [20].

Being already administrated for early detection of RHs [21] and follow-up after treatment [25], Smid et al. [26] used OCTA as an imaging tool for jRH classification in a single patient. However, data from a systematic application of OCTA technology to differentiate RH flow patterns in a large number of patients is not yet available. Therefore, this study aimed to correlate a growth pattern of RHs with their vascular structure defined by flow in OCTA

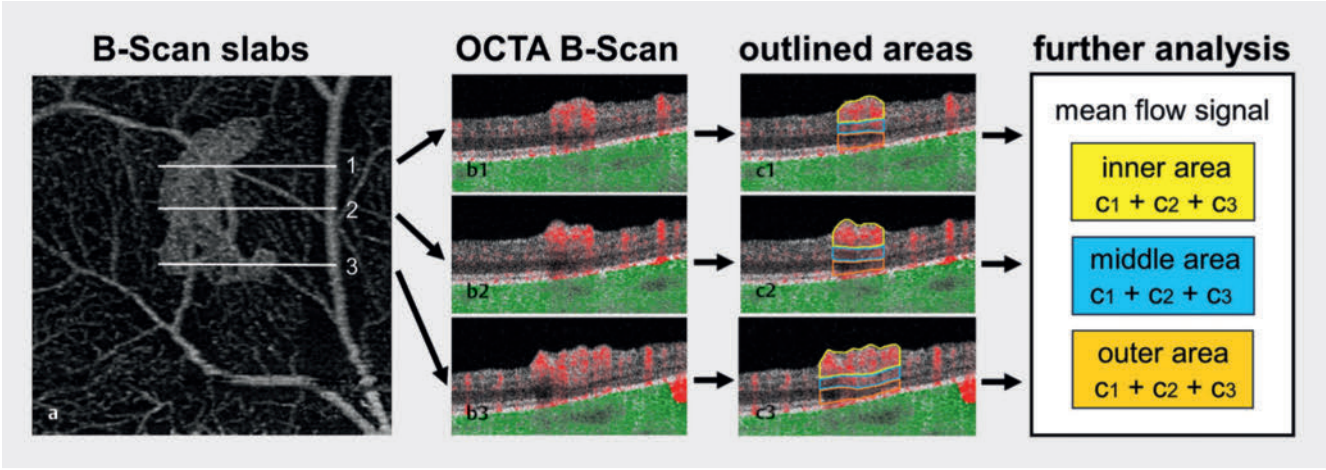

▶ **Fig. 1** Image processing. Representative optical coherence tomography angiography (OCTA) en face image (**a**), as well as three different OCTA B-scan slabs (**b**1–3) are illustrated. Graders outlined the inner, middle, and outer (outer nuclear layer and retinal pigment epithelium) area of the tumor (**c**1–3). The inner area (yellow) is located between the internal limiting membrane and halfway to the inner plexiform layer, the middle area (blue) between halfway to the inner plexiform layer and the outer nuclear layer, and the outer area (orange) between the outer nuclear layer and the retinal pigment epithelium.

and possibly facilitate a more individualized and targeted treatment in the future.

Methods

Study design

This was an observational, single-center, cross-sectional study approved by the institutional Ethics Committee of the University of Freiburg, Germany (ID number 360/19) and adhered to the tenets of the Declaration of Helsinki. Written informed consent was obtained from each subject.

Study population

A total of 217 consecutive patients with confirmed *VHL* gene mutation or clinically suspected VHLD due to VHLD in their family history or the presence of typical VHLD tumors were routinely examined at the Eye Center, Faculty of Medicine, University Freiburg, Germany, between January 2019 and February 2020. Patient characteristics such as sex, date of birth, and detected *VHL* gene mutation were documented.

Ophthalmological examination

All patients underwent a comprehensive ophthalmological examination, including best-corrected visual acuity, slit lamp microscopy, and dilated fundus examination including fundus photographs (FF450 fundus camera, Carl Zeiss, Meditec, Dublin, California, USA).

Optical coherence tomography angiography

All detected RHs underwent OCTA imaging using the PLEX Elite 9000 (Carl Zeiss, Meditec, Dublin, California, USA). The Zeiss PLEX Elite 9000 uses full spectrum SS-OCT with a light source wavelength of 1050 nm, an A-scan rate of 100 000 A-scans per second, and an A-scan depth of 3.0 mm in tissue (1536 pixels). The OCTA system utilizes the optical microangiography (OMAG) algorithm to decorrelate and visualize the blood flow signal within a blood vessel. A real-time image stabilizer (FastTrac Carl Zeiss, Meditec, Dublin, California, USA) minimized motion artefacts. Additionally, a 3 × 3-mm or, in case of a larger tumor size, a 6 × 6-mm volume scan with an axial scan depth of 2 mm each was obtained.

Lesion inclusion criteria

For further analysis, only images of primary treatment-naïve RHs that were completely captured in the scanned area were included. In case of a recurrence of a pretreated RH, scans taken at prior visits of the treatment-naïve RHs were added, if available. Only images of adequate signal strength of at least seven out of ten, as per the manufacturer's software, were included.

Image processing

As illustrated in ▶ **Fig. 1**, two graders (M. R., A. G.) outlined the inner, middle, and outer area (IA, MA, OA) in three B-scans of each RH using a Java and JavaScript custom-coded tool. Training and familiarization with the annotation tool was performed using OCTA images that were not included in the final grading. Two graders reached a consensus outline for each image. The total number of pixels depicting the flow signal (red pixels) in each outlined area (IA, MA, OA) was determined by the self-programmed tool. The mean flow signal of the corresponding outlined areas of the three B-scans of each RH was averaged for the further analysis.

Statistical analysis

GraphPad PRISM (GraphPad Software, version 8, San Diego, CA, USA) was used for statistical analysis. For descriptive data analysis, mean ± standard deviation (StD), median, as well as minimal and maximal values (range) were calculated. K-means cluster analysis, clustering for the three groups, was conducted including the

▶ **Table 1** K-means cluster analysis of the percentage of distribution of the flow signal measured in the entire tumor area over the inner, middle, and outer retinal layers. In accordance with the clinical picture, the clusters were assigned to the three tumor morphologies. The results are illustrated in ▶ **Fig. 2**. StD = standard deviation.

	Morphology	Percentage of distribution of the flow signal measured in the entire tumor area (%)								
		Inner retinal layers			Middle retinal layers			Outer retinal layers		
		Mean	StD	Range	Mean	StD	Range	Mean	StD	Range
Cluster 1	Exophytic	7.3	3.3	1.8–12.5	89.3	5.0	80.3–94.7	3.4	3.5	0–10.5
Cluster 2	Sessile	22.2	7.4	7.4–32.6	65.6	7.3	52.8–75.2	12.1	8.2	0.1–27.2
Cluster 3	Endophytic	65.4	5.7	54.4–72.2	26.6	4.9	19.9–35.0	8.0	6.1	0.1–21.5

three tumor areas – inner, middle, and outer retinal layers – as variables. According to their clinical representation, the three RH morphologies – endophytic, sessile, exophytic – were assigned to the three clusters. Due to the small number of cases, the difference in the *VHL* gene variant of the patients between the three RH morphology types was only described descriptively.

Results

Patient characteristics and detected retinal hemangioblastomas

Out of a total of 217 suspected VHLD patients, 201 patients were eligible and included in the study (male/female, 80/121 patients, 39.8/60.2%). Five patients were excluded due to neither clinical nor genetical confirmation of VHLD. Eleven patients were not included due to missing informed consent. The mean age of the cohort at the study examination was 39.5 ± 16.6 years (range from 7 to 82 years). Detailed information about the data collection is summarized in Supplemental Fig. 2.

There were 85 RHs detected in 49 patients. In relation to the complete study cohort (n = 201) this results in a mean of 0.42 ± 0.88 RH per patient (range 0 to 5). Forty of these 49 patients (81.6%) had at least one RH in one eye, and nine patients in both eyes (18.4%). Twenty-six (53.1%) patients had one active RH, 14 (28.6%) patients two RHs, six (12.2%) patients three RHs, two (4.1%) patients four RHs, and one (2.1%) patient five RHs. Fifty (58.8%) of the 85 RHs were located in the right eye, 35 (41.2%) in the left eye. Twenty-three RHs (27.1%) in 17 patients were located peripapillary (12 in the right eye, 11 in the left eye). Twelve patients had one jRH in one eye, four patients had two jRHs (one patient had one jRH in both eyes, three patients had two jRHs in one eye), and one patient had two jRHs in one eye and one jRH in the other eye. Of the 62 pRHs, 41 (66.1%) were located in or adjacent to a pretreated area and therefore considered as recurrent RHs and 21 (33.9%) were primary RHs.

OCTA imaging

Out of 44 detected primary RHs (21 pRHs, 23 jRHs), OCTA images of 24 lesions were suitable for further analysis. Suitable OCTA images of six recurrent RHs from a prior visit when the RH was treatment-naïve were available. Therefore, in total, 30 OCTA images of primary RH from 21 patients could be included in the data analysis. One patient had three primary RHs, seven patients two primary RHs, and 14 patients one primary RH. Eighteen of the 30 primary RHs were jRH (60%), and 12 were pRH (40%). Median signal intensity was 9 out of 10 (range 7 to 10 out of 10).

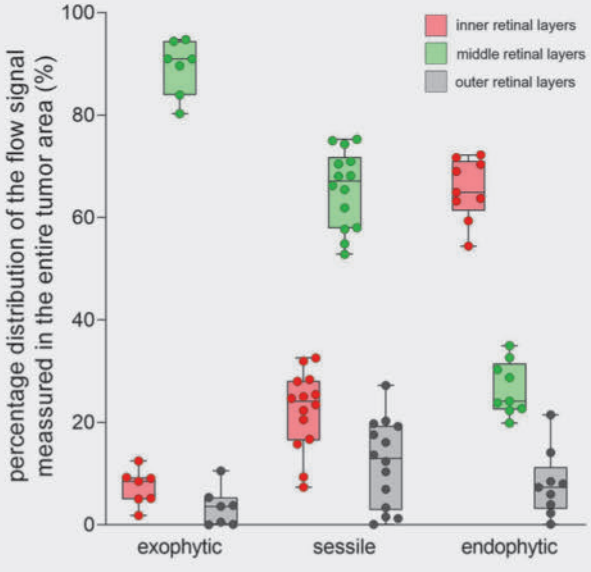

▶ **Fig. 2** K-means cluster analysis of the percentage of distribution of the flow signal measured in the entire tumor area over the inner, middle, and outer retinal layers. In accordance with the clinical picture, the clusters were assigned to the three tumor morphologies.

Morphology of juxtapapillary and peripheral retinal hemangioblastomas revealed by OCTA

The distribution of the flow signal in the IA, MA, and OA tumor area is shown in ▶ **Table 1** and **Fig. 2**. K-means cluster analysis separated seven exophytic (23.3%, 2 jRHs, 5 pRHs), nine endophytic (30%, 6 jRHs, 3 pRHs), and fourteen sessile (46.7%, 10 jRHs, 4 pRHs) growth patterns. Representative cases of endophytic, sessile, and exophytic jRHs and pRHs are illustrated in

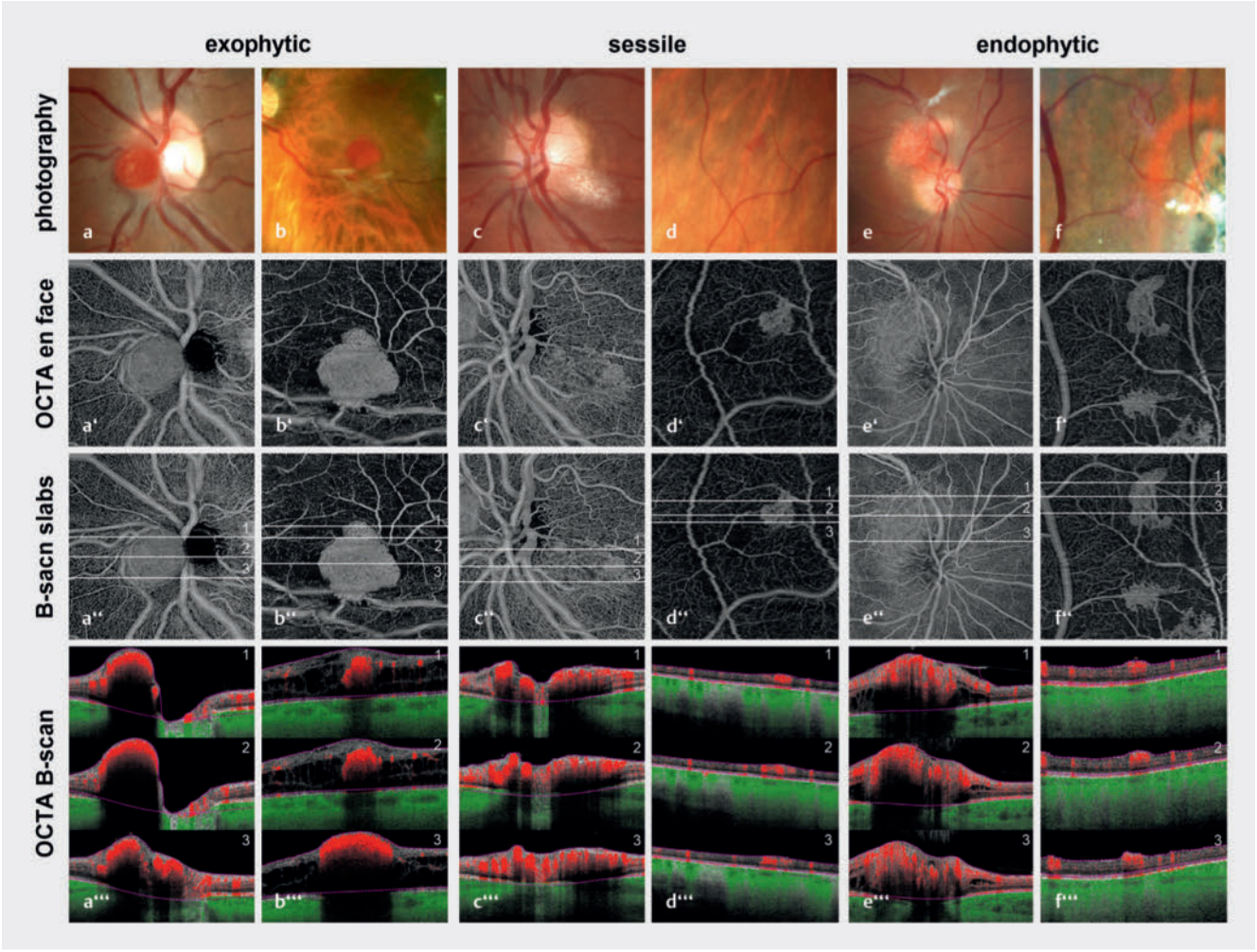

▶ **Fig. 3** Representative cases of exophytic, sessile, and endophytic juxtapapillary and peripheral retinal hemangioblastomas. Photography (**a**–**f**), optical coherence tomography angiography (OCTA) en face image (**a**′–**f**′), as well as the location of the B-scan slabs (**a**′′–**f**′′) and three different OCTA B-scan slabs (**a**′′′–**f**′′′) are illustrated. The clinical history of the shown cases is listed in Supplemental Table 1.

▶ **Fig. 3** Clinical data of these cases is provided in Supplemental Table 1.

Exophytic RHs were nodular, reddish, or orange colored (▶ **Fig. 3a** and **b**). In the OCTA en face image, these RHs showed a relative dense flow pattern and were clearly demarcated from the surrounding tissue (▶ **Fig. 3a**′ and **b**′). Their dense vascular signal is depicted in ▶ **Fig. 3a**′′′ and **b**′′′. The RHs displace the surrounding tissue, leading to a focally thickened perilesional retina and exudation with intraretinal fluid.

Sessile RHs were relatively flat and grayish, orange, or reddish in color (▶ **Fig. 3c** and **d**). In the OCTA en face image, these RHs showed a lesser flow signal than the exophytic lesion and were less clearly demarcated from the surrounding tissue due to vascular loops protruding on/from the edge of the RH (▶ **Fig. 3c**′ and **d**′). These RHs showed penetration of the surrounding tissue rather than a displacing growth pattern (▶ **Fig. 3c**′′′ and **d**′′′). The retina showed a rather flat configuration.

Endophytic RHs were reddish or orange colored and grew on the surface of the optic disc or retina (▶ **Fig. 3e** and **f**). In the OCTA en face image, a lower dense flow was detected in these RHs than in exophytic lesions. Like sessile tumors, endophytic RHs demonstrated less clearly demarcated borders from the surrounding tissue compared to the exophytic growth types (▶ **Fig. 3e**′ and **f**′). Hence, sessile and endophytic growth lesions showed similar features in OCTA en face scans. OCTA B-scans of endophytic RHs revealed a dense flow signal and thickening of the inner retinal layers (▶ **Fig. 3e**′′′ and **f**′′′). The RHs protruded into the vitreous cavity and progressively into deeper retinal layers.

Interestingly, one RH presented with two different patterns – exophytic and sessile – as shown in ▶ **Fig. 4** (case 6, Supplemental Table 1). Whether this RH was a single tumor with two different growth patterns, or two different tumors very closely localized to each other, cannot be distinguished by classic OCTA imaging. Therefore, only results of the nodular orange-colored part of the RH (▶ **Fig. 4c**, red) were included in the K-means cluster analysis. Of the eight patients having more than one primary RH, different growth patterns of these RHs could be identified in four patients.

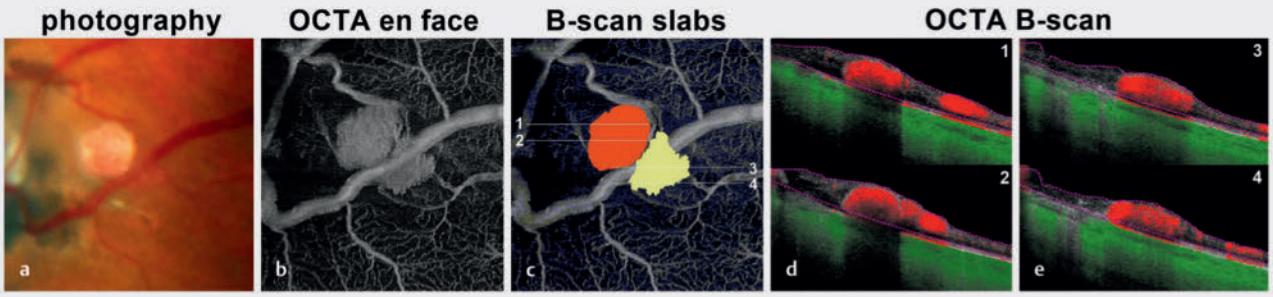

▶ **Fig. 4** Representative case of a peripheral retinal hemangioblastomas with different patterns. In the photography (**a**), a nodular orange-colored tumor is presented. In the optical coherence tomography angiography (OCTA) en face image (**b**, **c**), this part of the tumor is clearly demarcated from the surrounding tissue (**c**, red). However, in the OCTA en face image, a second part of the tumor is shown (**c**, yellow), which only appears in the photography (**a**) after closer inspection as flat and reddish. In the OCTA en face image (**b**, **c**), this part of the tumor shows a less clearly demarcation from the surrounding tissue due to vascular loops protruding at the edge of the tumor. The different morphologies are confirmed in the OCTA B-scans (**d**, **e**), showing a percentage of distribution of the flow signal as follows: 1.8% in the inner retinal layers, 94.4% in the middle retinal layers, 3.8% in the outer retinal layers (**c**, red); 31% in the inner retinal layers, 58.7% in the middle retinal layers, 10.3% in the outer retinal layers (**c**, yellow).

In the other four patients with more than one primary RH, the same growth patterns of the RH were detected.

Genetic subanalysis

Information regarding the *VHL* sequence variant was available for 17 patients. All three RH growth patterns were detected in patients with a truncating variant and patients with a single amino acid substitution. Five exophytic, five sessile, five endophytic RHs were detected in eleven patients with a truncating *VHL* gene variant, and two exophytic, three sessile, two endophytic RHs in six patients with a single amino acid substitution. Consequently, an association of the RH morphology and the genotype could not be detected.

Discussion

RHs remain a major cause of visual impairment or even loss of vision in patients with VHLD [8]. Since RHs are rare, there was a lack of a cohort demonstrating all three morphologies of jRHs and pRHs in one study. Including 201 patients, this study analyzes, for the first time, the flow distribution of juxtapapillary and peripheral RHs measured by OCTA, including all growth patterns, as illustrated in ▶ **Fig. 3**. Whether this additional information will lead to better therapeutic results remains to be seen.

Besides tumor size, tumor location (juxtapapillary or peripheral) and associated ocular findings, such as extent of subretinal fluid or retinal traction, the morphology of an RH is an important factor for the choice of optimal treatment [15]. Watchful waiting, off-label use of belzutifan [19], thermal laser photocoagulation, photodynamic therapy, cryotherapy, radiotherapy, and vitreoretinal surgery are described as possible treatment options for pRH [15]. Regarding jRH, vitreoretinal surgery is considered mainly for endophytic lesions due to their surgical accessibility [27], whereas intravitreal bevacizumab (with limited effectiveness) or verteporfin photodynamic therapy can be considered for sessile and exophytic RHs [28]. Since early detection of RH is important to minimize therapy as much as possible, all diagnostic possibilities including OCTA and fluorescence angiography (FAG) should be used to identify and classify the retinal tumor in VHLD as early as possible.

Different growth types of RHs have been described in the literature [15, 17, 18, 29]. Whereas some authors differentiate only between exophytic and endophytic growth types [29], the classification between exophytic, sessile, and endophytic growing RHs is more common [15, 17, 18] and therefore was used in our study. Since surgical removal of RHs is rarely necessary, only a few case reports describe the different growth patterns of RHs histologically [30]. Classification of tumor morphology is usually based upon the clinical picture of the tumor [17, 18], whereby FAG can provide additional information [17]. However, using only these methods of investigation, it is sometimes difficult to distinguish the different growth patterns.

As shown in previous studies, OCTA may serve as an additional tool for sensitive detection and monitoring of RHs [20, 25]. It also adds information on the flow properties of this vascular tumor, with a precision that cannot be achieved by invasive angiography. There are few case reports using OCTA for the classification of RH morphology [26]. Our study adds to this information in a systemic manner based on a large cohort of patients with VHDL. Endophytic and sessile growth types show flow signal distribution patterns, with the strongest flow signal in inner and middle retinal layers, respectively (see ▶ **Fig. 2**). Surprisingly, exophytic growth types show the most intense flow signal in the middle retinal layers instead of the outer retinal layers. This might be explained by the fact that, although using SS-OCTA, exophytic tumors show pronounced shadowing artifacts that usually appear after a small penetration depth into the tumor tissue due to their very dense flow (see ▶ **Fig. 3** and **4**). Therefore, the flow signal in deeper retinal layers cannot be detected reliably. The surrounding tissue is displaced rather than penetrated, leading to the nodular form of this tumor type and to a pronounced thinning of the middle and inner retinal layers in the tumor area. The increased flow signal of

the exophytic growth type therefore appears to be projected into middle retinal layers, although this tissue may have been completely pushed aside by the tumor and the measured flow signal could originate from the thickened outer retinal layers.

Little is known about the incidence of the different RH morphologies. In the study by McCabe et al. [18], 72 jRHs in 68 patients were examined. Fundus photographs were used to describe the growth type of the tumors, revealing a prevalence of about 30% for each growth pattern. Our study revealed that the sessile growth pattern is more common than endo- and exophytic lesions, including jRHs and pRHs (23.3% exophytic, 46.7% sessile, 30% endophytic). An association of the different tumor growth patterns with the underlying *VHL* gene mutation is not described in the literature yet and could also not be found in our study.

Our study is limited by the small number of RHs accessible for scanning, despite the large number of included subjects. Another important limitation is that inner, middle, and outer retinal layers in the area of the RH were manually outlined. Although the used slabs were blinded and outlining was performed by joint agreement of two different graders, there might be a selection bias in outlining the different layers. Further studies are needed using a higher number of primary tumors and, ideally, a grader-independent algorithm in analyzing the different flow signal patterns of the different RH growth patterns.

Conclusions

This study was able to correlate flow patterns measured by OCTA with all three RH morphologies – endophytic, sessile, exophytic – in jRHs as well as pRHs. Since the tumor morphology is an important factor in the choice of treatment, information from OCTA scans can contribute to a more adjusted therapy of RHs and therefore might help to improve the visual prognosis of patients with VHLD in the future.

CONCLUSION

Already known:

OCTA has been described as a useful tool for early RH detection, classification of single lesions, and post-treatment monitoring; however, its use in systematically classifying RH flow patterns across a broad patient sample remains unexplored. This study examines whether RH growth patterns correlate with flow patterns in OCTA.

Newly described:

There is a correlation between the flow patterns measured by OCTA and the three distinct RH morphologies–endophytic, sessile, and exophytic–in both juxtapapillary RHs and peripheral RHs. Given the critical role of tumor morphology in determining treatment approaches, OCTA scan data could support more tailored therapeutic strategies for RHs, potentially enhancing the visual prognosis for patients with VHLD in the future.

Conflict of Interest

The authors declare that they have no conflict of interest.

References

[1] Maher ER, Iselius L, Yates JR et al. Von Hippel-Lindau disease: a genetic study. J Med Genet 1991; 28: 443–447

[2] Maddock IR, Moran A, Maher ER et al. A genetic register for von Hippel-Lindau disease. J Med Genet 1996; 33: 120–127

[3] Evans DG, Howard E, Giblin C et al. Birth incidence and prevalence of tumor-prone syndromes: estimates from a UK family genetic register service. Am J Med Genet A 2010; 152A: 327–332

[4] Conway JE, Chou D, Clatterbuck RE et al. Hemangioblastomas of the central nervous system in von Hippel-Lindau syndrome and sporadic disease. Neurosurgery 2001; 48: 55–62

[5] Lonser RR, Glenn GM, Walther M et al. von Hippel-Lindau disease. Lancet 2003; 361: 2059–2067

[6] Schmidt D, Agostini HT. [Retinal angiomatosis – an ophthalmological challenge]. Klin Monbl Augenheilkd 2007; 224: 905–921

[7] Liang X, Shen D, Huang Y et al. Molecular pathology and CXCR4 expression in surgically excised retinal hemangioblastomas associated with von Hippel-Lindau disease. Ophthalmology 2007; 114: 147–156

[8] Chew EY. Ocular manifestations of von Hippel-Lindau disease: clinical and genetic investigations. Trans Am Ophthalmol Soc 2005; 103: 495–511

[9] Webster AR, Maher ER, Moore AT. Clinical characteristics of ocular angiomatosis in von Hippel-Lindau disease and correlation with germline mutation. Arch Ophthalmol 1999; 117: 371–378

[10] Salama Y, Albanyan S, Szybowska M et al. Comprehensive characterization of a Canadian cohort of von Hippel-Lindau disease patients. Clin Genet 2019; 96: 461–467

[11] Wittebol-Post D, Hes FJ, Lips CJ. The eye in von Hippel-Lindau disease. Long-term follow-up of screening and treatment: recommendations. J Intern Med 1998; 243: 555–561

[12] Maher ER, Yates JR, Harries R et al. Clinical features and natural history of von Hippel-Lindau disease. Q J Med 1990; 77: 1151–1163

[13] Neumann HP, Wiestler OD. Clustering of features of von Hippel-Lindau syndrome: evidence for a complex genetic locus. Lancet 1991; 337: 1052–1054

[14] Reich M, Jaegle S, Neumann-Haefelin E et al. Genotype–phenotype correlation in von Hippel-Lindau disease. Acta Ophthalmologica 2021; 99: e1492–e1500

[15] Singh AD, Shields CL, Shields JA. von Hippel-Lindau disease. Surv Ophthalmol 2001; 46: 117–142

[16] Binderup MLM, Stendell AS, Galanakis M et al. Retinal hemangioblastoma: prevalence, incidence and frequency of underlying von Hippel-Lindau disease. Br J Ophthalmol 2018; 102(7): 942–947

[17] Gass JD, Braunstein R. Sessile and exophytic capillary angiomas of the juxtapapillary retina and optic nerve head. Arch Ophthalmol 1980; 98 (10): 1790–1797

[18] McCabe CM, Flynn HW jr., Shields CL et al. Juxtapapillary capillary hemangiomas. Clinical features and visual acuity outcomes. Ophthalmology 2000; 107: 2240–2248

[19] Jonasch E, Donskov F, Iliopoulos O et al. Belzutifan for Renal Cell Carcinoma in von Hippel-Lindau Disease. N Engl J Med 2021; 385: 2036–2046

[20] Reich M, Glatz A, Boehringer D et al. Comparison of Current Optical Coherence Tomography Angiography Methods in Imaging Retinal Hemangioblastomas. Transl Vis Sci Technol 2020; 9: 12

[21] Lang SJ, Dreesbach M, Laich Y et al. Zeiss PLEX Elite 9000 Widefield Optical Coherence Tomography Angiography as Screening Method for Early

Detection of Retinal Hemangioblastomas in von Hippel-Lindau Disease. Transl Vis Sci Technol 2024; 13(2): 8

[22] Kashani AH, Chen CL, Gahm JK et al. Optical coherence tomography angiography: A comprehensive review of current methods and clinical applications. Prog Retin Eye Res 2017; 60: 66–100

[23] Wang F, Zhang Q, Deegan AJ et al. Comparing imaging capabilities of spectral domain and swept source optical coherence tomography angiography in healthy subjects and central serous retinopathy. Eye Vis (Lond) 2018; 5: 19

[24] Reich M, Boehringer D, Rothaus K et al. Swept-source optical coherence tomography angiography alleviates shadowing artifacts caused by subretinal fluid. Int Ophthalmol 2020; 40: 2007–2016

[25] Lang SJ, Cakir B, Evers C et al. Value of Optical Coherence Tomography Angiography Imaging in Diagnosis and Treatment of Hemangioblastomas in von Hippel-Lindau Disease. Ophthalmic Surg Lasers Imaging Retina 2016; 47: 935–946

[26] Smid LM, van Overdam KA, Davidoiu V et al. Classification and treatment follow-up of a juxtapapillary retinal hemangioblastoma with optical coherence tomography angiography. Am J Ophthalmol Case Rep 2019; 15: 100472

[27] Kreusel KM, Bechrakis NE, Neumann HP et al. Pars plana vitrectomy for juxtapapillary capillary retinal angioma. Am J Ophthalmol 2006; 141: 587–589

[28] Saitta A, Nicolai M, Giovannini A et al. Juxtapapillary retinal capillary hemangioma: new therapeutic strategies. Med Hypothesis Discov Innov Ophthalmol 2014; 3: 71–75

[29] Garcia-Arumi J, Sararols LH, Cavero L et al. Therapeutic options for capillary papillary hemangiomas. Ophthalmology 2000; 107: 48–54

[30] Darr JL, Hughes RP jr., McNair JN. Bilateral peripapillary retinal hemangiomas. A case report. Arch Ophthalmol 1966; 75: 77–81